Automated Skin Cancer Detection and Classification using Cat Swarm Optimization with a Deep Learning Model

Vijay Arumugam Rajendran
Department of Computer Science, Government Arts and Science College, India
vijaynew@gmail.com (corresponding author)

Saravanan Shanmugam
Department of Computer and Information Science, Annamalai University, India
aucissaran@gmail.com

Received: 28 November 2023 | Revised: 9 December 2023 | Accepted: 13 December 2023

 DOI: https://doi.org/10.48084/etasr.6681

ABSTRACT

The application of Computer Vision (CV) and image processing in the medical sector is of great significance, especially in the recognition of skin cancer using dermoscopic images. Dermoscopy denotes a non-invasive imaging system that offers clear visuals of skin cancers, allowing dermatologists to analyze and identify various features crucial for lesion assessment. Over the past few years, there has been an increasing fascination with Deep Learning (DL) applications for skin cancer recognition, with a particular focus on the impressive results achieved by Deep Neural Networks (DNNs). DL approaches, predominantly CNNs, have exhibited immense potential in automating the classification and detection of skin cancers. This study presents an Automated Skin Cancer Detection and Classification method using Cat Swarm Optimization with Deep Learning (ASCDC-CSODL). The main objective of the ASCDC-CSODL method is to enforce the DL model to recognize and classify skin tumors on dermoscopic images. In ASCDC-CSODL, Bilateral Filtering (BF) is applied for noise elimination and U-Net is employed for the segmentation process. Moreover, the ASCDC-CSODL method exploits MobileNet for the feature extraction process. The Gated Recurrent Unit (GRU) approach is used for the classification of skin cancer. Finally, the CSO algorithm alters the hyperparameter values of GRU. A wide-ranging simulation was performed to evaluate the performance of the ASCDC-CSODL model, demonstrating the significantly improved results of the ASCDC-CSODL model over other approaches.

Keywords-skin cancer; dermoscopic images; deep learning; cat swarm optimization; computer-aided diagnosis

I. INTRODUCTION

Today, skin cancer is an increasingly common type of cancer. There are several types of skin carcinoma [1]. Melanoma is the most prevalent cancer in both males and females [2]. As the initial indicators of skin cancer may not always be visible, diagnostic assessments typically rely on the expertise of dermatologist specialists. For untrained physicians, an automatic diagnosis system is a crucial tool for a highly accurate diagnosis [3]. Apart from that, the diagnosis of skin carcinoma with the naked eye is rarely generalizable and extremely subjective. Therefore, there is a need to improve automated classification systems to be even more accurate, cost-effective, and faster [4]. Furthermore, the implementation of such automatic diagnostic systems can efficiently reduce mortality from skin cancers and help medical systems and patients [5].

Several medical professionals use Artificial Intelligence (AI) for clinical diagnoses to improve diagnosis decision-making processes [6]. However, the currently available AI research has neglected existing evidence of development, accurate evaluation, and sufficient reports of predictive errors in such fields. Computer-aided diagnosis techniques could rapidly, reliably, and regularly diagnose different diseases [7]. Computer-aided diagnosis provides options for accurate and low-cost detection or protection from developed tumors. Individual organ diseases are usually diagnosed using various imaging techniques, such as MRI, X-rays, and PET [8]. Initially, methods such as clinical screening, dermoscopy image analysis, Computed Tomography (CT), etc., are used to visually diagnose skin lesions. Dermatologists with few skills have exhibited minimal accuracy in the diagnosis of skin lesions [9]. The techniques for practitioners to analyze and evaluate lesion images are complex, error-prone, time-consuming, and subjective [10]. The use of Machine Learning (ML) has offered considerable developments in prediction systems and computer-aided diagnosis for detecting skin cancer.

This study presents an Automated Skin Cancer Detection and Classification method using Cat Swarm Optimization with Deep Learning (ASCDC-CSODL). The main objective of ASCDC-CSODL is to apply DL on dermoscopic images to recognize and classify skin tumors. This method uses Bilateral Filtering (BF) for the noise elimination process and U-Net for the segmentation process. Moreover, the ASCDC-CSODL method exploits MobileNet for the feature extraction process. The classification of skin cancer is performed using a Gated Recurrent Unit (GRU), and the CSO algorithm adjusts the hyperparameter values of the GRU. A wide-ranging simulation was performed to evaluate the performance of the proposed ASCDC-CSODL method.

II. LITERATURE REVIEW

In [11], a lightweight skin carcinoma detection technique was presented, depending on the principle of fine-grained categorization and using two categories of training models, negative and positive model sets, as input into the feature extraction segment (lightweight CNNs). In [12], an innovative DL-based architecture was proposed for the multi-categorization of skin carcinoma categories (basal cell cancer, benign keratosis, melanocytic nevi, and melanoma). This SCDNet integrated VGG16 with CNNs to classify many types of skin cancer. In [13], a DNN was used with fine-tuning training and enhanced learning performance on dermoscopic images to detect skin cancer. Fine-tuning and Transfer Learning (TL) were implemented for faster training on restricted trained datasets. In [14], the Intelligent Multi-Level Thresholding with DL (IMLT-DL) method was proposed, which relied on skin cancer segmentation and classification models using dermoscopic images. This method combined inpainting and top-hat filtering methods for the preprocessing of dermoscopic images. In addition, MFOs with multilevel Kapur thresholds rely on segmentation processes that are included in identifying diseased areas. Finally, the classifier used the Gradient Boosting Tree (GBT) technique.

In [15], a DCNN-based method was presented to classify skin carcinoma types with greater accuracy. An EfficientNet framework based on TL models was applied, which learned highly complicated and fine-grained models from skin cancer images by automatic scaling width, resolution, and depth of networks. In [16], an innovative CNN scheme was developed based on atrous convolutions for automated skin lesion segmentation. This design relies on the idea of dilated or atrous convolution, which is efficient for semantic segmentation. The DNN was implemented from scratch using many building blocks that contained leakyReLU, batch normalization, and convolutional layers, along with fine-tuned hyperparameters to provide enhanced performance. In [17], an ensemble method was proposed that used Swin-Transformer and EfficientNetV2S to detect the initial focal region of skin cancer, having the benefit of identifying dark regions in the images. In [18], a Fractal Neural Network-Based Galactic Swarm Optimization (FNN–GSO) was proposed, involving four components and using adaptive watershed segmentation. Then, the DWT-GLCM and FNN-GSO approaches were used for feature extraction and classification.

In [19], the Sand CSO with Deep Transfer Learning Method (SCSODTL-SCC) was proposed, where segmentation and classification processes used a hybrid Deep Belief Network (DBN) model incorporating U2Net and NASNetLarge-based feature extractors, while the SCSO model was used for the tuning process. In [20], a model was presented that used auxiliary function smoothing, built with a prevalent local minimizer, and smoothed using Bezier curves to determine threshold values in images related to melanoma skin cancer. In [21], an automated diagnostic system was introduced using a support vector machine, which was an improved iteration of the fluid search optimization approach rooted in chaos theory, contributing to a faster convergence speed. In [22], the Cat Swarm-Intelligent Generative RNN (CS-IGRNN) approach was presented, which employed the Weiner Filter (WF) for image preprocessing. The features were extracted through Gabor Filter Bank (GFB) processing, and the use of CS-IGRNN was suggested as a prospective solution for the categorization of cancer images.

Despite the advances in skin cancer detection techniques, several drawbacks are evident in existing methodologies. Some methods exhibit computational complexity due to the integration of multiple algorithms, potentially impacting real-time processing efficiency and resource utilization. Additionally, challenges persist in achieving a balance between sensitivity and specificity, which are crucial for minimizing false positives or negatives in skin cancer diagnoses. Furthermore, the reliance on extensive computational resources and large datasets for training can pose practical challenges, especially in resource-constrained medical settings.

III. THE PROPOSED MODEL

This study designed an ASCDC-CSODL approach to apply DL on dermoscopic images to classify and recognize skin cancer. In ASCDC-CSODL, the BF method is used for the noise elimination process and U-Net is employed for the segmentation process. Additionally, the proposed method uses MobileNet for feature extraction. Also, the classification of skin tumors is performed using the GRU technique. Finally, CSO adjusts the hyperparameter values of the GRU. Figure 1 illustrates the workflow of the proposed ASCDC-CSODL method.

A. Image Preprocessing

The BF technique was used to preprocess the input images. This method decreases noise but maintains the fine and edge details of the images [23]. It accomplishes this by taking into account either spatial distance or intensity similarity among pixels. An important stage of the BF approach is:

- Determine a window or kernel of a certain size.
- For the overall image pixels, compute the weighted average of its nearby pixels depending on either spatial distance or intensity similarity.
- The weights can be defined by a spatial Gaussian function and an intensity Gaussian function. The spatial Gaussian function ensures that nearby pixels take a superior weight,

and the intensity Gaussian function ensures that pixels with the same intensity take a superior weight.

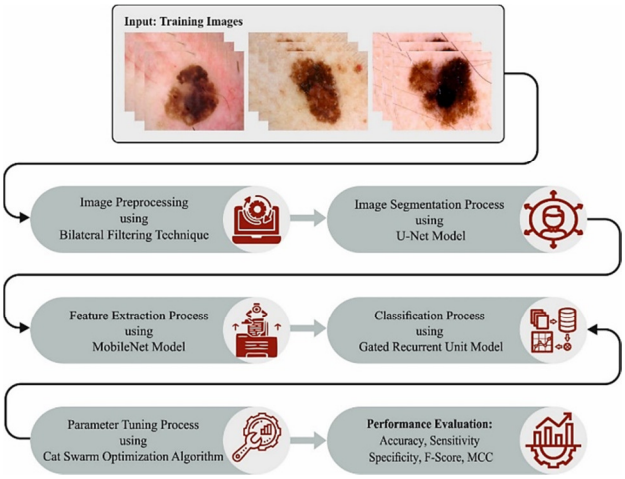

Fig. 1. Workflow of the ASCDC-CSODL approach.

B. Image Segmentation

The U-Net approach was used to segment the dermoscopic images. U-Net is the most widely used segmentation model, depending on the encoder-decoder neural structure and the use of skip connections [24]. This method receives an image as input during encoding, exploits more than one layer of convolution, ReLU activation, max-pooling, and encompasses the data into hidden space. The only difference between the plain encoder-decoder and the U-Net method is the usage of skip connections to transmit the data in the higher-resolution layer of encoded to decoded, which might assist in better capturing smaller details. CNUReject demonstrates the overall framework of U-Net. U-Net exploits the following loss function to train like other neural segmentation models:

$$\mathcal{L}_{Unet} = \sum_{x\in\Omega} \omega\,(x)\log\left(p_{\ell(x)}(x)\right) \quad (1)$$

where $\ell: \Omega \rightarrow \{1, \ldots, K\}$, $\Omega \subset \mathbb{Z}^2$, and K indicates the overall amount of class labels. While applying the binary cross entropy, $K = 2$. Furthermore, the softmax is described as $p_k(x) = \exp\left(a_k(x)\right)/\sum_{k'=1}^{K} \exp\left(a_{k'}(x)\right)$, where $a_k(x)$ denotes the activation in the feature channel K.

Furthermore, in a network that has different convolution layers, the primary weight considerably affects the achievement. Consequently, roughly the unit variance of the primary weight of the network feature map was carried out effectively. With the ReLU and U-Net convolutional layers, employing a Gaussian distribution with SD of $\sqrt{2/N}$ is the best solution, where N denotes the number of nodes received from a single neuron.

C. Feature Extraction

The MobileNet architecture was used for feature extraction. It is a shallow DNN technique that is optimal for decreasing computational cost and time [25]. MobileNet alternates depth-wise convolution with standard convolutions to minimize model processing and size. Employing a factorizing system termed depthwise convolutional, a normal convolution was separated into 2 convolutions: point-wise and depth-wise. A 1×1-dimensional convolution is point-wise. Point-wise convolution tries to join, whereas depth-wise tries to filter. The procedure of depth-wise distinguishable convolutions is the outcome of more depth-wise and point-wise convolutions. In addition to the upper layer, the structure of MobileNet contained separable convolutions.

D. Image Classification using Optimal GRU Model

The GRU model was used to effectively recognize and classify skin tumors. The GRU framework has adaptive memory and forgets the hidden unit [26]. The reset gate was computed as:

$$r_j = \sigma([W_r x]_j + [u_r h_{<f-1>}]_j) \quad (2)$$

where σ refers to the activation function of the logistic sigmoid, $[*]_j$ represents the j^{th} module of the vector, x denotes the input, and h_{t-1} denotes the preceding moment to allow the status. The matrices W_r and U_r are identified weighted matrices. The upgrade gate was computed by:

$$z_j = \sigma([W_z x]_j + [u_{z<t-1>} h]_j) \quad (3)$$

where h_j demonstrates the target cell state vector that was measured by:

$$h_j^{<t>} = z_j \odot h_j^{<t-1>} + (1 - z_j) \odot h_j^{<t>} \quad (4)$$

$$h_{j<t>} = \tanh\left([Wx]_j + \left[U\left(\odot h_{\langle t-1\rangle}\right)\right]_j\right) \quad (5)$$

where $\odot$ stands for multiplication performed on a per-element basis. Finally, the hyperparameter selection of the GRU model was performed by the CSO algorithm. CSO is established dependent on the cat's performance. The CSO contains 2 sub-modes: seeking and tracing [27].

1) Seeking Mode

During the SCO procedure, the seeking mode was projected to model the cat in resting time and then alertly search nearby places for its next moves. Four important aspects can be executed in the seeking mode: Count of Dimension to Change (CDC), Seeking Range of the selected Dimension (SRD), Seeking Memory Pool (SMP), and Self-Position Consideration (SPC). SMP determines the seeking memory size of all cats that represent any point sorted by a cat. SRD denotes the mutative ratio to the elected dimension. Once the dimension is chosen for mutation, the difference between new and old values cannot be outside the range determined by SRD. CDC means that several dimensions are different. Each factor plays a vital role in this mode. SPC is a Boolean value and represents if the point where the cat was previously standing is going to be the best Candidate Point (CP) to move to. SPC could not stimulate the SMP value. The seeking mode is explained as follows:

- Create j copies of the current location of cat_k, where $j = SMP$. When SPC is true, consider (SMP-1), and then keep the current position as most candidates.

- For all the copies, based on *CDC*, arbitrarily select positive or negative *SRD* percent of the existing values and exchange them with old ones.
- Compute the value of fitness (*FS*) of every *CP*.
- If every *FS* could not accurately be equivalent, compute the choosing probability of all the CPs based on (6). Otherwise, set every electing probability of all the CPs that are equal to 1.
- Arbitrarily choose the point to move in the CPs, and exchange the location of cat_k:

$$P_i = \frac{|FS_i - FS_b|}{FS_{\max} - FS_{\min}}, \text{ where } 0 < i < j \quad (6)$$

The Fitness Function's (FF) purpose is to determine the minimal outcome, assume $FS_b = FS_{max}$, else, $FS_b = FS_{min}$.

2) Tracing Mode

Tracing mode methods the occurrence of cats from tracing goals. If a cat switches to the tracing mode, it starts moving based on the individual velocities of all the dimensions. The tracing mode is performed as:

- Upgrade the velocity to all the dimensions $v_{k,d}(z)$ for cat_k at the present iteration based on:

$$v_{k,d}(z) = v_{k,d}(z-1) + r_1 \cdot c_1 \cdot [x_{best,d}(z-1) - x_{k,d}(z-1)], d = 1,2,\dots,M \quad (7)$$

- Verify if the velocity is in the maximal velocity range. When the novel velocity is out of range, it can be adjusted to the range.
- Upgrade the location of cat_k based on:

$$x_{k,d}(z) = x_{k,d}(z-1) + v_{k,d}(z) \quad (8)$$

where $x_{best,d}(z\text{-}1)$ depicts the cat position that takes an optimal value of fitness at the prior iteration, and $x_{k,d}(z\text{-}1)$ denotes the location of cat_k. In the preceding iteration, c_1, r_1 indicate the constant and the arbitrary value within [0, 1]. *CSO* illustrates an FF for higher classifier outcomes. It controls a positive numeral to exemplify the good solution of candidate performance. The error rate of the minimized classifier can be regarded as a FF:

$$fitness(x_i) = \frac{No.\ of\ misclassified\ instances}{Total\ No.\ of\ instances} \times 100 \quad (9)$$

IV. PERFORMANCE VALIDATION

The proposed ASCDC-CSODL method was evaluated on the ISIC2017 and HAM10000 datasets. Figure 2 shows some sample images. The dataset contains 2000 samples under 3 classes. The proposed method was simulated using Python 3.6.5 on an i5-8600K, GeForce 1050Ti 4GB, 250GB SSD, 1TB HDD, and 16GB RAM PC. The parameter setup was: learning rate: 0.01, activation: ReLU, epoch count: 50, dropout: 0.5, and batch size: 5.

ASCDC-CSODL was compared with previous methods, and Figure 3 shows the comparison results in the ISIC2017 dataset [28]. The NB, MSVM, KELM, MobileNet, and DenseNet169 methods achieved poor results. The MAFCNN-SCD method has revealed substantial performance with $accu_y$, $sens_y$, $spec_y$, and F_{score} of 92.22, 77.07, 88.67, and 83.05%, respectively, while the proposed ASCDC-CSODL method showed even better results with $accu_y$, $sens_y$, $spec_y$, and F_{score} of 97.44, 93.42, 97.01, and 94.63%, respectively.

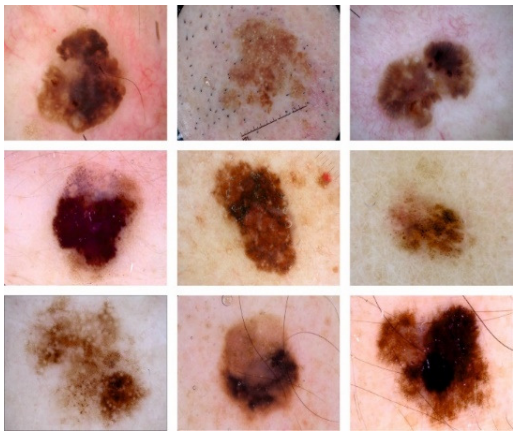

Fig. 2. Sample mages.

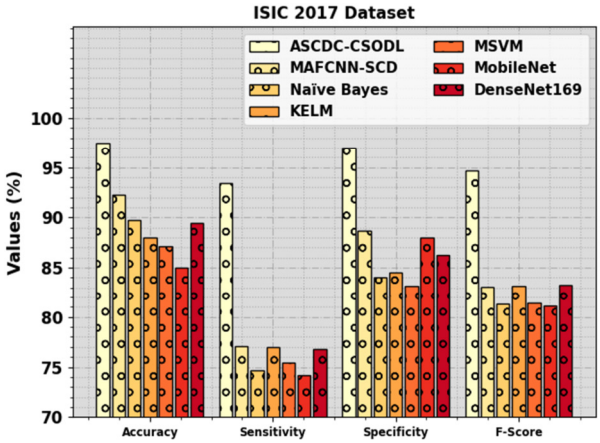

Fig. 3. Relative output of ASCDC-CSODL and other methods in the ISIC2017 dataset.

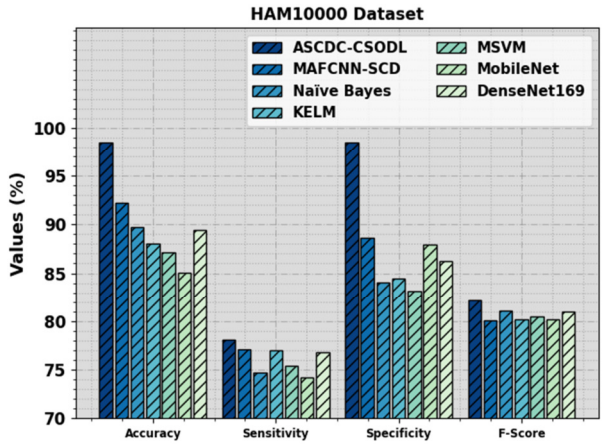

Fig. 4. Relative output of the ASCDC-CSODL and other methods in the HAM10000 dataset.

Figure 4 shows a comparison of ASCDC-CSODL with MAFCNN-SCD, NB, MSVM, KELM, MobileNet, and DenseNet169 methods in the HAM10000 dataset. The results show that NB, MSVM, KELM, MobileNet, and DenseNet169 reported comparably poor performance. The MAFCNN-SCD method has exposed substantial outputs with $accu_y$, $sens_y$, $spec_y$, and F_{score} of 92.22, 77.07, 88.67, and 80.05, respectively. ASCDC-CSODL provided the best results with $accu_y$, $sens_y$, $spec_y$, and F_{score} of 98.48, 78.06, 98.45, and 82.18%, respectively. Therefore, the ASCDC-CSODL method can be used effectively for skin cancer detection and classification purposes.

V. CONCLUSION

This study introduced the ASCDC-CSODL approach, which used a DL model to classify and recognize skin cancer in dermoscopy images. In this approach, the noise elimination process involved the application of the BF method, the segmentation process was carried out using U-Net, and feature extraction was performed using MobileNet. Skin tumor classification was performed through GRU, with hyperparameter values adjusted by the CSO technique. The effectiveness of the ASCDC-CSODL approach was validated through simulations, exhibiting improved results of 97.44% and 98.48% in two datasets over other approaches. Future research could focus on enhancing the ASCDC-CSODL approach by addressing its computational complexity and refining its ability to generalize across diverse skin conditions. Furthermore, exploring the integration of additional advanced image processing or DL techniques may contribute to overcoming current limitations and improving overall performance.

REFERENCES

[1] M. Attique Khan, M. Sharif, T. Akram, S. Kadry, and C.-H. Hsu, "A two-stream deep neural network-based intelligent system for complex skin cancer types classification," *International Journal of Intelligent Systems*, vol. 37, no. 12, pp. 10621–10649, 2022, https://doi.org/10.1002/int.22691.

[2] E. Gomathi, M. Jayasheela, M. Thamarai, and M. Geetha, "Skin cancer detection using dual optimization based deep learning network," *Biomedical Signal Processing and Control*, vol. 84, Jul. 2023, Art. no. 104968, https://doi.org/10.1016/j.bspc.2023.104968.

[3] M. Nawaz *et al.*, "Skin cancer detection from dermoscopic images using deep learning and fuzzy k-means clustering," *Microscopy Research and Technique*, vol. 85, no. 1, pp. 339–351, 2022, https://doi.org/10.1002/jemt.23908.

[4] C. Srilakshmi, L. Laxmi, and N. Ramakrishnaiah, "Dung Beetle Optimization Algorithm with Multi-modal Deep Learning based Skin Cancer Classification on Dermoscopic Images." Research Square, Jul. 05, 2023, https://doi.org/10.21203/rs.3.rs-2995167/v2.

[5] A. Ech-Cherif, M. Misbhauddin, and M. Ech-Cherif, "Deep Neural Network Based Mobile Dermoscopy Application for Triaging Skin Cancer Detection," in *2019 2nd International Conference on Computer Applications & Information Security (ICCAIS)*, Riyadh, Saudi Arabia, Feb. 2019, pp. 1–6, https://doi.org/10.1109/CAIS.2019.8769517.

[6] S. Lafraxo, M. E. Ansari, and S. Charfi, "MelaNet: an effective deep learning framework for melanoma detection using dermoscopic images," *Multimedia Tools and Applications*, vol. 81, no. 11, pp. 16021–16045, May 2022, https://doi.org/10.1007/s11042-022-12521-y.

[7] Y. Dahdouh, A. A. Boudhir, and M. B. Ahmed, "A New Approach using Deep Learning and Reinforcement Learning in HealthCare: Skin Cancer Classification," *International Journal of Electrical and Computer Engineering Systems*, vol. 14, no. 5, pp. 557–564, Jun. 2023, https://doi.org/10.32985/ijeces.14.5.7.

[8] K. Rajeshkumar, C. Ananth, and N. Mohananthini, "Blockchain-Assisted Homomorphic Encryption Approach for Skin Lesion Diagnosis using Optimal Deep Learning Model," *Engineering, Technology & Applied Science Research*, vol. 13, no. 3, pp. 10978–10983, Jun. 2023, https://doi.org/10.48084/etasr.5594.

[9] N. B. Hiremath and P. Dayananda, "Differential Gene Expression Analysis of Non-Small Cell Lung Cancer Samples to Classify Candidate Genes," *Engineering, Technology & Applied Science Research*, vol. 13, no. 2, pp. 10571–10577, Apr. 2023, https://doi.org/10.48084/etasr.5770.

[10] N. Behar and M. Shrivastava, "A Novel Model for Breast Cancer Detection and Classification," *Engineering, Technology & Applied Science Research*, vol. 12, no. 6, pp. 9496–9502, Dec. 2022, https://doi.org/10.48084/etasr.5115.

[11] M. Li, C. Han, and F. Fahim, "Skin Cancer Diagnosis Based on Support Vector Machine and a New Optimization Algorithm," *Journal of Medical Imaging and Health Informatics*, vol. 10, no. 2, pp. 356–363, Feb. 2020, https://doi.org/10.1166/jmihi.2020.2889.

[12] A. Naeem, T. Anees, M. Fiza, R. A. Naqvi, and S.-W. Lee, "SCDNet: A Deep Learning-Based Framework for the Multiclassification of Skin Cancer Using Dermoscopy Images," *Sensors*, vol. 22, no. 15, Jan. 2022, Art. no. 5652, https://doi.org/10.3390/s22155652.

[13] V. Venugopal, N. I. Raj, M. K. Nath, and N. Stephen, "A deep neural network using modified EfficientNet for skin cancer detection in dermoscopic images," *Decision Analytics Journal*, vol. 8, Sep. 2023, Art. no. 100278, https://doi.org/10.1016/j.dajour.2023.100278.

[14] G. Reshma *et al.*, "Deep Learning-Based Skin Lesion Diagnosis Model Using Dermoscopic Images," *Intelligent Automation & Soft Computing*, vol. 31, no. 1, pp. 621–634, 2022, https://doi.org/10.32604/iasc.2022.019117.

[15] J. S M, M. P, C. Aravindan, and R. Appavu, "Classification of skin cancer from dermoscopic images using deep neural network architectures," *Multimedia Tools and Applications*, vol. 82, no. 10, pp. 15763–15778, Apr. 2023, https://doi.org/10.1007/s11042-022-13847-3.

[16] R. Kaur, H. GholamHosseini, R. Sinha, and M. Lindén, "Automatic lesion segmentation using atrous convolutional deep neural networks in dermoscopic skin cancer images," *BMC Medical Imaging*, vol. 22, no. 1, May 2022, Art. no. 103, https://doi.org/10.1186/s12880-022-00829-y.

[17] K. Shehzad *et al.*, "A Deep-Ensemble-Learning-Based Approach for Skin Cancer Diagnosis," *Electronics*, vol. 12, no. 6, Jan. 2023, Art. no. 1342, https://doi.org/10.3390/electronics12061342.

[18] S. P. Karuppiah, A. Sheeba, S. Padmakala, and C. A. Subasini, "An Efficient Galactic Swarm Optimization Based Fractal Neural Network Model with DWT for Malignant Melanoma Prediction," *Neural Processing Letters*, vol. 54, no. 6, pp. 5043–5062, Dec. 2022, https://doi.org/10.1007/s11063-022-10847-0.

[19] C. S. S. Anupama, S. Yonbawi, G. Jose Moses, E. Laxmi Lydia, S. Kadry, and J. Kim, "Sand Cat Swarm Optimization with Deep Transfer Learning for Skin Cancer Classification," *Computer Systems Science and Engineering*, vol. 47, no. 2, pp. 2079–2095, 2023, https://doi.org/10.32604/csse.2023.038322.

[20] I. A. Masoud Abdulhamid, A. Sahiner, and J. Rahebi, "New Auxiliary Function with Properties in Nonsmooth Global Optimization for Melanoma Skin Cancer Segmentation," *BioMed Research International*, vol. 2020, Apr. 2020, Art. no. e5345923, https://doi.org/10.1155/2020/5345923.

[21] L. Wei, K. Ding, and H. Hu, "Automatic Skin Cancer Detection in Dermoscopy Images Based on Ensemble Lightweight Deep Learning Network," *IEEE Access*, vol. 8, pp. 99633–99647, 2020, https://doi.org/10.1109/ACCESS.2020.2997710.

[22] A. Shukla, G. K. Shyam, R. Shree, and R. Naaz, "Skin Cancer Identification using Cat Swarm-Intelligent Generative RNN Algorithm," *International Journal of Intelligent Systems and Applications in Engineering*, vol. 11, no. 8s, pp. 447–454, Jul. 2023.

[23] F. Spagnolo, P. Corsonello, F. Frustaci, and S. Perri, "Design of Approximate Bilateral Filters for Image Denoising on FPGAs," *IEEE*

Access, vol. 11, pp. 1990–2000, 2023, https://doi.org/10.1109/ACCESS.2022.3233921.

[24] N. Saeedizadeh, S. Minaee, R. Kafieh, S. Yazdani, and M. Sonka, "COVID TV-Unet: Segmenting COVID-19 chest CT images using connectivity imposed Unet," *Computer Methods and Programs in Biomedicine Update*, vol. 1, Jan. 2021, Art. no. 100007, https://doi.org/10.1016/j.cmpbup.2021.100007.

[25] S. Akter, H. Shahriar, and A. Cuzzocrea, "Autism Disease Detection Using Transfer Learning Techniques: Performance Comparison Between Central Processing Unit vs Graphics Processing Unit Functions for Neural Networks," in *2023 IEEE 47th Annual Computers, Software, and Applications Conference (COMPSAC)*, Torino, Italy, Jun. 2023, pp. 1084–1092, https://doi.org/10.1109/COMPSAC57700.2023.00164.

[26] Y. Duan, Y. Liu, Y. Wang, S. Ren, and Y. Wang, "Improved BIGRU Model and Its Application in Stock Price Forecasting," *Electronics*, vol. 12, no. 12, Jan. 2023, Art. no. 2718, https://doi.org/10.3390/electronics12122718.

[27] P.-W. Tsai, J.-S. Pan, S.-M. Chen, B.-Y. Liao, and S.-P. Hao, "Parallel Cat Swarm Optimization," in *2008 International Conference on Machine Learning and Cybernetics*, Kunming, China, Jul. 2008, vol. 6, pp. 3328–3333, https://doi.org/10.1109/ICMLC.2008.4620980.

[28] M. Obayya *et al.*, "Henry Gas Solubility Optimization Algorithm based Feature Extraction in Dermoscopic Images Analysis of Skin Cancer," *Cancers*, vol. 15, no. 7, Jan. 2023, Art. no. 2146, https://doi.org/10.3390/cancers15072146.